university of groningen

University of Groningen

University Medical Center Groningen

Experimental and modeling studies on the absorption of NO in aqueous ferrous EDTA solutions

Gambardella, F; Alberts, MS; Winkelman, JGM; Heeres, EJ; Alberts, Michel S.; Heeres, H.J.

IMPORTANT NOTE: You are advised to consult the publisher's version (publisher's PDF) if you wish to cite from it. Please check the document version below.

Document Version
Publisher's PDF, also known as Version of record

Link to publication in University of Groningen/UMCG research database

Experimental and Modeling Studies on the Absorption of NO in Aqueous Ferrous EDTA Solutions

Francesca Gambardella, Michel S. Alberts, Jos G. M. Winkelman, and Erik J. Heeres*

Department of Chemical Engineering, Stratingh Institute, Rijks Universiteit Groningen, Nijenborgh 4, 9747 AG, Groningen, The Netherlands

This work describes an experimental and modeling study on an industrial relevant process (i.e., the absorption of NO in aqueous $Fe^{II}(EDTA)$ solutions) to accurately determine the equilibrium constant of the reaction in the temperature range of 299–329 K. The experiments were carried out in a stirred cell contactor using a pH of 7 and an initial $Fe^{II}(EDTA)$ concentration of 7–9 mol/m^3. A dynamic reactor model was developed to describe the experimental absorption profiles. Mass transfer effects were taken into account using the penetration theory for mass transfer. Excellent fits were obtained between measured and modeled profiles when assuming that the reaction takes place in the instantaneous regime. The following temperature dependence for the K value was obtained: $K = \exp((4702/T) - 8.534)$. Dynamic reactor modeling not only allowed calculation of the equilibrium constants of the reaction but also provided accurate values for the ratio of the diffusivity of $Fe^{II}(EDTA)$ and NO (r_P) at various temperatures. This ratio is of extreme importance for the design of a reactive NO absorption unit and could be expressed as: $r_P = -1.775 \times 10^{-4}T^2 + 0.11T - 16.93$.

1. Introduction

NO_x gas emissions from human activities contribute to about 6% of the greenhouse gases released to the atmosphere.[1] Various technologies have been developed in the past decades to reduce these emissions, ranging from combustion modification to flue gas treatment.[2] Combustion modifications have resulted in NO reduction levels of about 60%, which is not sufficient to meet the emission limits set by international regulations. Flue gas treatment concepts seem to be more promising, and higher NO reduction levels have been demonstrated as compared to combustion modifications. The most widely used flue gas treatment technology is selective catalytic reduction, which is based on the reaction of NO gas with ammonia using a heterogeneous catalyst to form nitrogen and water. Drawbacks of this method are the relatively high costs involved and environmental concerns on the use of ammonia.[3] A large number of alternative flue gas treatment technologies have been proposed and studied on various scales.[2] Promising concepts are wet removal technologies. Here, the NO gas is absorbed in an aqueous solution with a suitable reactant. Metal chelate solutions rapidly react with the absorbed NO gas to form stable metal–nitrosyl complexes. Absorption rates using these metal complexes are significantly higher than in pure water. Particularly, Fe^{II} chelates based on ethylenediaminetetraacetic acid (EDTA) and related compounds such as NTA (nitrilotriacetic acid) were proven to be very effective, see reaction given in eq 1:[4,5]

$$Fe^{II}(EDTA) + NO \rightleftharpoons Fe^{II}(EDTA)(NO) \qquad (1)$$

It should be noted that the actual ferrous complex is a seven coordinate species, viz., $Fe^{II}(EDTA)(H_2O)$, and

that the produced NO complex is formally an Fe^{III} species, $Fe^{III}(EDTA)(NO^-)$. However, to be consistent with earlier literature on the reaction, throughout this paper, these species will be denoted as shown in reaction 1.

To be economically viable, efficient methods are required to regenerate the metal–chelate solutions. Various strategies have been developed like electrochemical regeneration, reduction of the bound NO with sulfite ions to nitrogen and sulfate, and reactions with metallic powder.[6-8]

Recently, a novel biotechnological approach has been described to regenerate the loaded iron–chelate solution.[9] In this so-called BiodeNOx process, the loaded iron–chelate solution is brought in intimate contact with specific microorganisms that convert the nitrosyl complex back to the original $Fe^{II}(EDTA)$ complex and N_2 gas. $Fe^{III}(EDTA)$, formed in the absorption process due to the presence of oxygen in the flue gas, is reduced to the original $Fe^{II}(EDTA)$ solution:

$$12Fe^{III}(EDTA) + C_2H_5OH + 3H_2O \rightarrow$$
$$12Fe^{II}(EDTA) + 2CO_2 + 12H^+ \quad (2)$$
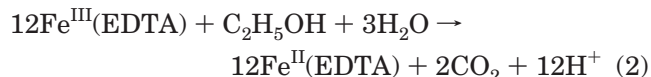
As part of a larger program to determine the technical and economical feasibility of this novel NO removal process, we have studied the absorption of NO gas in aqueous $Fe^{II}(EDTA)$ solutions in more detail. The reaction of NO with $Fe^{II}(EDTA)$ has been studied by various research groups using different reactor configurations and experimental conditions. An overview is given in Table 1.

All studies conclude that the reaction is first order in both reagents. However, the resulting kinetic and thermodynamic data show considerable spreading (Table 2). One reason for this scatter is probably the high rate of the reaction of NO with $Fe^{II}(EDTA)$, which may result in severe mass transfer limitation of both NO and

---

* To whom correspondence should be addressed. Fax: +31 50 363 4479. E-mail: h.j.heeres@rug.nl.

Table 1. Overview of Experimental Studies on NO Absorption in Aqueous Fe^{II}(EDTA) Solution

reactor	T (K)	pH	$C_{Fe^{II}}$ (mol/m^3)	C_{NO^I} (mol/m^3)	reference
bubble column stirred cell	288–308	2–10	10–30	$(4-30) \times 10^{-4}$	Teramoto et al.[10]
bubble column	311–343	1–6	8–36	$(8.3-24) \times 10^{-4}$	Hishinuma and Kaji[11]
stirred cell	298	1.5–10	10–50	$(1.4-20) \times 10^{-4}$	Sada et al.[12]
bubble column	308	6–8	10	17×10^{-4}	Sada et al.[13]
stirred cell	298–353	7	10–50	$(5-50) \times 10^{-4}$	Yih and Lii[14]
stirred cell	298–348	2–10	10–50	$(0.5-7.9) \times 10^{-4}$	Huasheng and Wenchi[15]
bubble column	277–363	na^a	10–100	$(2.0-8.0) \times 10^{-4}$	Nymoen et al.[16]
stirred reactor	298	<1	4–12	1.9	Shy et al.[17]
stirred cell	293–333	7–8	5–100	0.13–0.49	Demmink[18]
stopped flow, flash photolysis pulse radiolysis	298	4.9–7.2	2	0–1.8	Schneppensieper et al.[19–21]

^{a} na = not provided in original literature source.

Table 2. Kinetic and Equilibrium Constants Cited in the Literature for the Reaction of NO with Fe^{II}(EDTA)

T (K)	pH	k_1 (m^3/(mol·s))	k_{-1} (1/s)	K (m^3/mol)	reference
298	4.6–8.0	1.7×10^5		1.5×10^3	Teramoto et al.[10]
313	7.6			5.5×10^2	
311	3			3.48×10^3	Hishinuma et al.[11]
328	3			8.59×10^3	
243	3			3.39×10^3	
298	1.5–2.5	3.29×10^4			Sada et al.[12]
298	7	1.23×10^5			
298	9.5–10	1.04×10^5			
308	6–8			9.90×10^2	Sada et al.[13]
298	7	1.24×10^5			Yih and Lii[14]
313	7	1.35×10^5			
333	7	1.43×10^5			
353	7	1.47×10^5			
288	na^a			2.18×10^3	Huasheng and Wenchi[15]
298	na^a			1.53×10^3	
308	na^a			7.82×10^2	
328	na^a			5.31×10^2	
348				2.52×10^2	
293	na^a			1.7×10^3	Nymoen et al.[16]
313	na^a			3.9×10^3	
333	na^a			1.1×10^2	
298	5.1	$>6.0 \times 10^5$	>60		Shy et al.[17]
298	5	2.4×10^5	91	2.1×10^3	Schneppensieper et al.[19–21]

^{a} na = not provided in original literature source.

Fe^{II}(EDTA). So far, only the study of Demmink[18] has taken into account the effect of mass transfer limitation of the Fe^{II}(EDTA) species on the overall rate of the absorption process. They have shown that, even under low NO partial pressure, the absorption rate is completely limited by ferrous mass transfer. However, they assumed the reaction to be irreversible. Recent mechanistic studies by Schneppensieper et al.,[19–21] using pulse radiolysis and stopped flow techniques, have unequivocally proven that the reaction has to be treated as reversible.

The target of the present study is the determination of the equilibrium constants for the reaction of NO with Fe^{II}(EDTA) in a range of conditions that are relevant to the BiodeNOx process (i.e., $298 < T < 328$ K, $[NO]_G = 0-1000$ vppm, $1 < [Fe^{II}(EDTA)] < 50$ mol/m^3), taking into account the reversibility of the reaction and mass transfer limitation of both NO and Fe^{II}(EDTA) in the solution. Subsequent studies to determine the influence of the simultaneous absorption of oxygen are in progress and will be published in forthcoming papers.

2. Experimental Section

2.1. Chemicals. FeCl$_2$·4H$_2$O (p.a.), titriplex (p.a.), and Na$_2$CO$_3$ were obtained from Merck; NaOH (33% in water) was from Boom; CeSO$_4$·4H$_2$O (>99%) was from

Table 3. Dimensions and Characteristics of the Stirred Cell Contactor

total reactor volume (m^3)	1.245×10^{-3}
interfacial area (m^2)	7.79×10^{-3}
gas impeller (m)	six-bladed turbine $d = 6 \times 10^{-2}$
N$_s$ liquid stirrer (min^{-1})	100
N$_s$ gas impeller (min^{-1})	2000

Acros; and NO (1008 vppm in N$_2$), N$_2$O (>99%), and N$_2$ (>99.99%) were from Hoek Loos. Reverse osmosis water was applied to prepare the various solutions.

2.2. Experimental Setup. The kinetic experiments were carried out in a stirred cell reactor consisting of glass, equipped with four glass baffles. The reactor could be operated in batch as well as continuous mode with respect to the gas phase and in batch mode with respect to the liquid. A stainless steel turbine impeller was used to stir the gas phase, while a magnetic stirrer (2 cm) in combination with an external magnetic drive was used for the liquid phase. The double wall of the reactor allowed the use of water to regulate the temperature in the reactor (Julabo, MV basis). Typical dimensions of the stirred cell contactor are given in Table 3.

Temperature (PT-100) and pressure transducers (Trafag, ECO 2.5 A) were used to determine the temperature and pressure during an experiment. The NO concentration in the outlet was measured using an NO
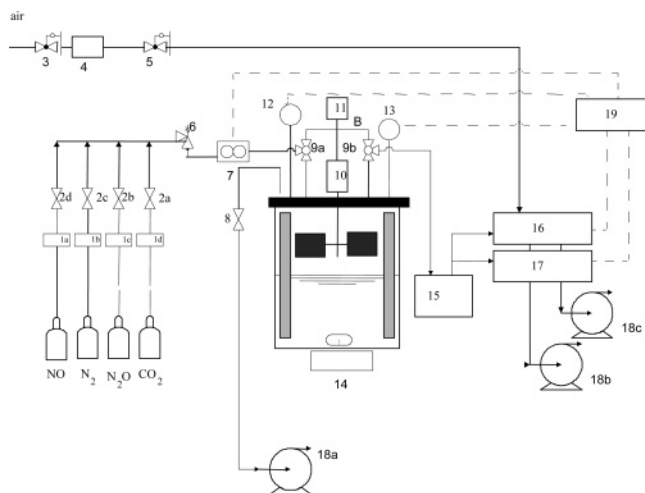
Figure 1. Schematic representation of the experimental setup. 1a−d: mass-flow controllers; 2a−d, 6, 8: open/close valves; 3−5: air valves and filter; 7: digital flowmeter; 9a,b: three-way valve; B: bypass; 10: magnetic coupling; 11: motor; 12: temperature transducer; 13: pressure transducer; 14: magnetic drive; 15: cold trap; 16: NO analyzer; 17: O₂ analyzer; 18a−c: vacuum pump; 19: pc.

analyzer (Thermo Electron-Model 10). The NO analyzer was calibrated before and after every experiment using an NO gas mixture of known concentration. The NO analyzer, the temperature, and the pressure transducer were connected to a computer equipped with an NI-4351 PCI (National Instrument) data acquisition card. The reactor setup is schematically represented in Figure 1.

2.3. Preparation of Fe^{II}(EDTA) Solutions. Aqueous solutions of Fe^{II}(EDTA) are extremely air-sensitive and should be handled under a protective nitrogen atmosphere. The Fe^{II}(EDTA) solution was prepared by dissolving a predetermined amount of titriplex (EDTA) in degassed water (150 mL). The turbid solution turned transparent when the pH was increased from 4 to 9 by carefully addition of some drops of a 4 M NaOH solution. The appropriate amount of FeCl$_2$·4H$_2$O (Fe:EDTA ratio = 1:1.2 mol/mol) was added to the EDTA solution, giving a slightly green, clear solution with a pH of about 3. Next, the solution was diluted further with degassed water to 900 mL. At this stage, the pH was adjusted to the desired value by the addition of a 4 M NaOH solution. Finally, degassed water was added to adjust the total volume to 1 L.

2.4. Physical Absorption Experiment. Physical absorption experiments were performed using N$_2$O gas. The reactor was operated in batch mode, with respect to both the gas and the liquid phase. The reactor was filled with the iron−chelate solution and thoroughly degassed for about 15 min. Next, the reactor was filled with N$_2$O gas until the desired pressure was reached. The experiment was initiated by starting the gas and liquid stirrers. The pressure inside the reactor was measured using a pressure transducer and recorded by a computer.

2.5. Determination of the Gas-Phase Mass Transfer Coefficients. Gas-phase mass transfer coefficients at various experimental conditions were obtained by measuring the evaporation rate of water into an airstream. The reactor outlet was connected to 2 cold traps in series cooled with ice. The amount of evaporated liquid was obtained by determining the weight increase of the cold traps.

2.6. Equilibrium Absorption Experiments. During the reactive absorption experiments, the liquid phase was operated in batch mode while the gas phase was operated continuously. The reactor was filled with the appropriate amount of solution and degassed under vacuum for about 15 min. After degassing, the reactor was filled with nitrogen gas until atmospheric pressure was reached. The reactor was heated to the desired temperature. A gas mixture of NO in N$_2$ was initially bypassed around the reactor to the analysis unit. The NO concentration in the gas stream was regulated using two mass flow controllers, and the composition of the mixture gas was determined using the NO analyzer. The actual absorption was started by closing the bypass valves and admitting the NO in nitrogen mixture gas to the reactor. The NO concentration of the outlet flow was measured as a function of the time. The experiment was terminated when the outlet NO concentration was equal to the inlet value. Desorption experiments were performed by switching the gas stream from NO/N$_2$ to pure N$_2$, after establishment of equilibrium. The NO concentration in the outlet stream was monitored as a function of time.

2.7. Determination of the Fe^{II} Content in the Solution. The concentration of Fe^{II} in the solution was determined before every absorption experiments by titration with a 0.1 M Ce(SO$_4$)$_2$ solution, using 0.025 M ferroine as indicator.[22] To obtain reproducible results, the iron−chelate sample was diluted with an approximate 10-fold volume of sulfuric acid (2−4 kmol/m^3) and subsequently degassed by adding approximately 1 g of NaHCO$_3$ prior to the titration.

3. Theory

A general equation for the flux of NO, here denoted as component A, in a reactive gas−liquid system may be given by:[23]

$$J_A = \left(\frac{1}{mk_L E_A} + \frac{1}{k_G}\right)^{-1}\left(C_{A,G}{}^b - \frac{C_{A,L}{}^b}{m}\right) \qquad (3)$$

Various theoretical mass transfer models have provided expressions for the enhancement factor for the absorption process described in eqs 4 and 5:

$$A_G \rightarrow A_L \qquad (4)$$

$$A_L + B_L \leftrightarrow P_L \qquad (5)$$

Onda et al.[24] obtained an expression for E_A using the film theory. In the instantaneous regime, E_A can be expressed as[23]

$$E_A = E_{A,\infty} = 1 + r_P\frac{KC_{B,L}{}^b}{1 + \frac{r_P}{r_B}KC_{A,L}{}^i} \qquad (6)$$

Related expressions using the penetration theory have been derived.[25,26] In case the reactive absorption process takes place in the instantaneous regime, the following approximate solution may be applied:[23]

$$E_A = E_{A,\infty} = \left(1 + r_P\frac{KC_{B,L}{}^b}{1 + \frac{r_P}{r_B}KC_{A,L}{}^i}\right)\left(\frac{1}{r_B}\right)^{0.5} \qquad (7)$$
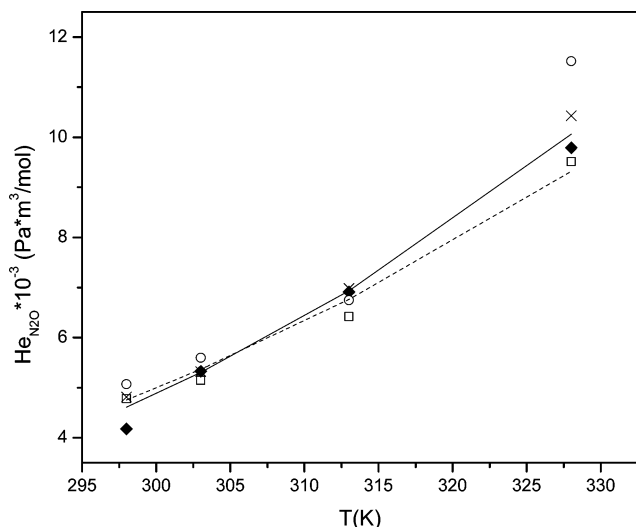
Figure 2. Henry coefficient of N_2O in $Fe^{II}(EDTA)$ solution as a function of the temperature. $\bigcirc$: $[Fe^{II}(EDTA)] = 100$ mol/m^3; $\times$: $[Fe^{II}(EDTA)] = 75$ mol/m^3; $\blacklozenge$: $[Fe^{II}(EDTA)] = 50$ mol/m^3; $\square$: $[Fe^{II}(EDTA)] = 25$ mol/m^3. The dotted line represents the results obtained by Wubs[29] for $[Fe^{II}(EDTA)] = 100$ mol/m^3. The continuous line represents eq 11.

4. Physical Properties and Mass Transfer Coefficients

4.1. Solubility of NO in $Fe^{II}(EDTA)$ Solutions. Direct determination of the solubility of NO in iron−EDTA solutions is not possible due to the reactive nature of the system. However, indirect determination is possible when performing absorption experiments with N_2O instead of NO. According to Demmink,[18] the Henry coefficient of NO may be obtained using:

$$He_{NO} = A_g (He_{NO,w}) \left(\frac{He_{N_2O}}{He_{N_2O,w}} \right) \qquad (8)$$

Here, He is the Henry coefficient defined as

$$He_A = \frac{p_A}{C_{A,L}^i} \qquad (9)$$

A_g is a gas-specific salting out parameter[18] that is close to unity for NO at 298 K, whereas the solubility of N_2O in water ($He_{N_2O,w}$) is given by Versteeg and van Swaaij.[27] The solubility of NO in pure water ($He_{NO,w}$) is given by Fogg and Gerrard.[28]

The Henry coefficient of N_2O in an iron−chelate solution was determined experimentally using the reactor set up as described in the Experimental Section. The absorption experiments were carried out in a batch mode, both for the gas and the liquid phase. The pressure in the reactor was measured as a function of the time, allowing calculation of the He coefficient using:

$$He = \frac{p^\infty - p_w}{p^0 - p^\infty} \frac{RTV_L}{V_G} \qquad (10)$$

Figure 2 shows the experimentally obtained solubilities of N_2O in solutions of $Fe^{II}(EDTA)$ solutions at various temperatures (298−328 K) and Fe concentrations (25−100 mol/m^3). As expected, the He coefficient increases at higher temperatures. However, a clear
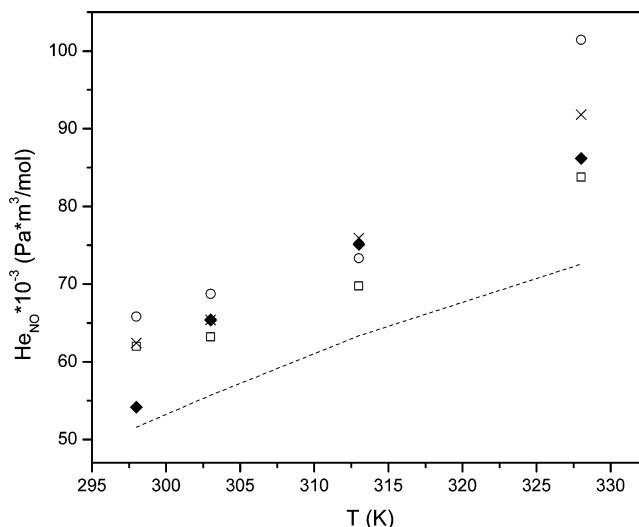
Figure 3. Henry coefficient of NO in $Fe^{II}(EDTA)$ solutions. $\bigcirc$: $[Fe(EDTA)] = 100$ mol/m^3; $\times$: $[Fe(EDTA)] = 75$ mol/m^3; $\blacklozenge$: $[Fe(EDTA)] = 50$ mol/m^3; $\square$: $[Fe(EDTA)] = 25$ mol/m^3. The dotted line represents the He coefficient for NO in water.[28]

relation between the He_{N_2O} and the concentration of the iron chelate appears to be absent in this concentration range. When assuming that the He is not affected for Fe^{II} loadings below 100 mol/m^3, the following relation for the temperature dependency of the He coefficient of N_2O may be calculated:

$$He_{N_2O} = 2.35 \times 10^7 \, e^{-2544/T} \qquad (11)$$

These results are in fairly good agreement with the results obtained by Wubs:[29]

$$He_{N_2O} = 7.51 \times 10^6 \, e^{-2195/T} \qquad (12)$$

Subsequently, the Henry coefficients for NO in $Fe^{II}(EDTA)$ solutions at various temperatures were calculated using eq 8. The results are represented in Figure 3.

4.3. Diffusion Coefficients. The values for the diffusion coefficient of NO in water at various temperatures may be estimated using the following relation:[30]

$$D_{NO,w} = 0.00398 \, e^{-3.5 \times 10^4/RT} \qquad (13)$$

A correction for the fact that the reaction takes place in an electrolyte solution consisting of $Fe^{II}(EDTA)$ instead of pure water is applied using a relation given by Ho et al.:[31]

$$D_{NO} = D_{NO,w} \left(\frac{\mu_w}{\mu_{Fe(EDTA)}} \right)^{0.62} \qquad (14)$$

Here, $\mu_w/\mu_{Fe(EDTA)}$ represents the relative viscosity of the $Fe^{II}(EDTA)$ solution, which was measured by Wubs[29] for a $[Fe^{II}(EDTA)]$ of 100 mol/m^3.

4.3. Mass Transfer Coefficients. The liquid-phase mass transfer coefficients for NO at different temperatures and $Fe^{II}(EDTA)$ concentrations were calculated from physical absorption experiments of pure N_2O. The k_L values for N_2O were obtained from the
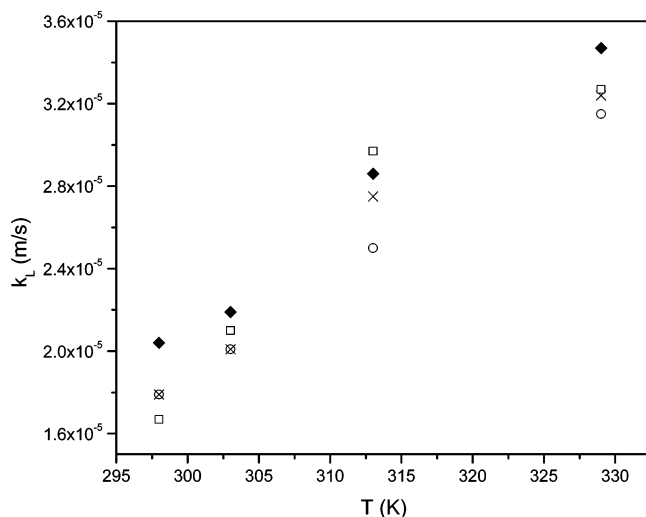
Figure 4. Mass transfer coefficient of NO in $Fe^{II}(EDTA)$ solutions. ○: [Fe(EDTA)] = 100 mol/m³; ×: [Fe(EDTA)] = 75 mol/m³; ◆: [Fe(EDTA)] = 50 mol/m³; □: [Fe(EDTA)] = 25 mol/m³.

pressure versus time curves using:

$$(k_L)_{N_2O}at = \left(\frac{\alpha}{\alpha+1}\right)\ln\left(\frac{p_{N_2O}{}^0}{(\alpha+1)p_{N_2O} - \alpha p_{N_2O}{}^0}\right) \quad (15)$$

with

$$\alpha = \frac{V_G He}{V_L RT} \quad (16)$$

According to the penetration theory, the k_L values for NO are related to those of N_2O by the following expression:[23]

$$(k_L)_{NO} = (k_L)_{N_2O}\sqrt{\frac{D_{NO}}{D_{N_2O}}} \quad (17)$$

The experimental values of the mass transfer coefficients for NO as a function of the temperature are given in Figure 4.

The gas-phase mass transfer coefficients at various conditions were obtained by measuring the rate of evaporation of pure water into an airstream.[32] The k_G values of water in air were calculated using a balance for the vapor content of the carrier gas stream combined with the weight of the condensed vapor:

$$F_G p_w{}^{out} = k_G a V_L(p_w{}^{sat} - p_w)\left(1 - \frac{p_w}{p_{tot}}\right) \quad (18)$$

$$\frac{W}{M_w t} = \frac{F_G p_w}{\left(1 - \frac{p_w}{p_{tot}}\right)RT} \quad (19)$$

According to the penetration theory, the gas-phase mass transfer coefficient of NO in N_2 (k_{gNO-N_2}) is related to the experimentally determined value for water in air by

$$k_{gNO-N_2} = k_{gw-air}\sqrt{\frac{D_{NO-N_2}}{D_{w-air}}} \quad (20)$$
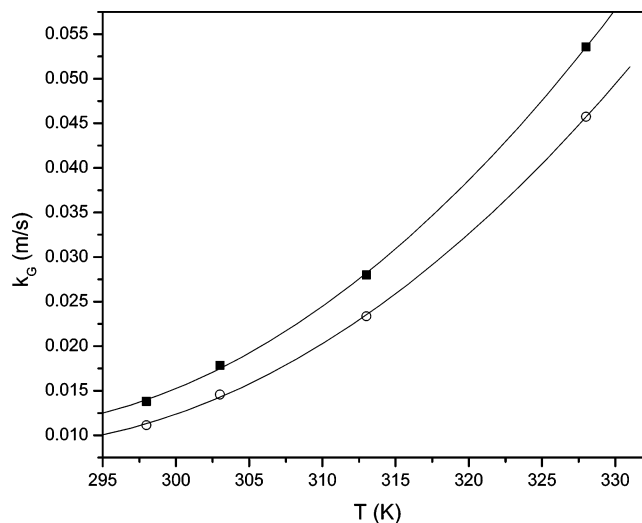
Figure 5. Measured k_G values for water vapor in air (○) and calculated values for NO in N_2 (■).

Table 4. Overview of Experiments

|	experiment				
	1	2	3	4[a]	5
temp (K)	299	304	314	313	329
liquid vol (10⁴ m³)	2.05	1.65	1.65	1.45	2.45
gas vol (10³ m³)	1.04	1.08	1.08	1.10	1.00
[Fe^{II}(EDTA)] (mol/m³)	8.1	8.8	7.9	7.4	8.5
gas flow (10⁶ mol/m³)	8.74	8.85	9.11	9.12	9.57
[NO]$_{in}$ (10² mol/m³)	4.13	4.07	3.95	3.95	3.76

[a] Duplicate of experiment 3.

where D_{w-air} is provided by Janssen and Warmoes-kerken,[33] and the D_{NO-N_2} is estimated using the relation given by Reid et al.[34] The experimental values for the k_g of water in air and the derived values for the k_g of NO in nitrogen are represented in Figure 5.

5. Results and Discussion

5.1. Determination of the Equilibrium Constant of the Reaction at Equilibrium Conditions. Equilibrium experiments were performed to determine the equilibrium constant at various temperatures and a fixed pH of 7. The reaction was allowed to proceed until the concentration in the outlet stream was equal to the inlet concentration. Reaction times of up to 7 h were required to establish equilibrium. A summary of the experiments is given in Table 4.

A typical experimental profile is represented in Figure 6. A first stage with rapid concentrations changes is observed followed by second phase where a slow increase of the NO concentration up to the inlet concentration is observed. In the second stage, the actual reaction occurs and equilibrium is established.

Evidence that the reaction should indeed be treated as an equilibrium reaction was obtained by performing desorption experiments. The feed composition was changed from a mixture gas of NO in N_2 to pure N_2 gas after saturation of the solution with NO and establishment of equilibrium. A rapid drop in the NO concentration in the outlet was observed to about 300 vppm, followed by a stage with a slow decrease. The latter stage suggests that NO is formed by the backward reaction and subsequently transferred to the gas phase. These findings clearly prove that the reaction should be treated as an equilibrium reaction.
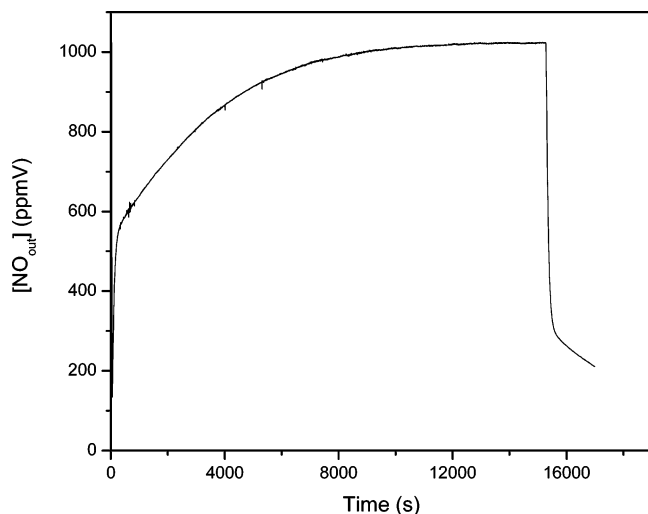
Figure 6. Absorption of NO in $Fe^{II}(EDTA)$ solutions in the stirred cell contactor followed by desorption. $[Fe(EDTA)] = 7.4$ mol/m^3, $[NO]_{in} = 1000$ vppm, $T = 313$ K, pH = 7.

The equilibrium constant for the reaction (eq 1) is given by

$$K = \frac{C_{P,L}}{C_{A,L}C_{B,L}}\bigg|_{\text{at equilibrium}} \tag{21}$$

The concentration of the components in the liquid at equilibrium can be rewritten as:

$$C_{P,L} = \frac{F_G}{V_L}\left(C_{A,G}{}^{in}t - \int_0^{t_{end}} C_{A,G}\,\mathrm{d}t\right) - \left(\frac{V_G}{V_L} + m\right)C_{A,G}{}^{in} \tag{22}$$

$$C_{A,L} = mC_{A,G}{}^{in} \tag{23}$$

$$C_{B,L} = C_{B,L}{}^0 - C_{P,L} \tag{24}$$

The values of the equilibrium constant at different temperatures were determined using eqs 21–24, and the results are given in Figure 7.

A linear relation ($R^2 = 0.996$) was observed. The equilibrium constants from previous studies have also been provided in Figure 7. It is clear that there is a considerable spread in the data. As mentioned in the Introduction, most of the experimental studies carried out so far have not properly taken into account mass transfer limitations of NO and/or the iron chelate species, which is, according to our findings, of prime importance to obtain reliable results.

5.2. Dynamic Reactor Modeling. The values of the equilibrium constants may also be obtained from the experimentally determined absorption profiles (Figure 6). The absorption profiles were modeled assuming that the reaction between NO and $Fe^{II}(EDTA)$ is reversible (see previous section); that the gas and liquid phase in the stirred cell reactor are ideally mixed, which was confirmed by RTD experiments; and that the absorption process takes place in the instantaneous regime. The latter assumption can be justified by some very basic calculations using the so-called Hatta number (see Supporting Information). Using literature data on the diffusivity[30] and the reaction rate at 298 K[21] together with our experimental k_L and $C_{Fe(EDTA)}$, the calculated Ha number is $(5-6) \times 10^3$. The observed enhancement factors were always $<10^3$. Therefore, for all experi-
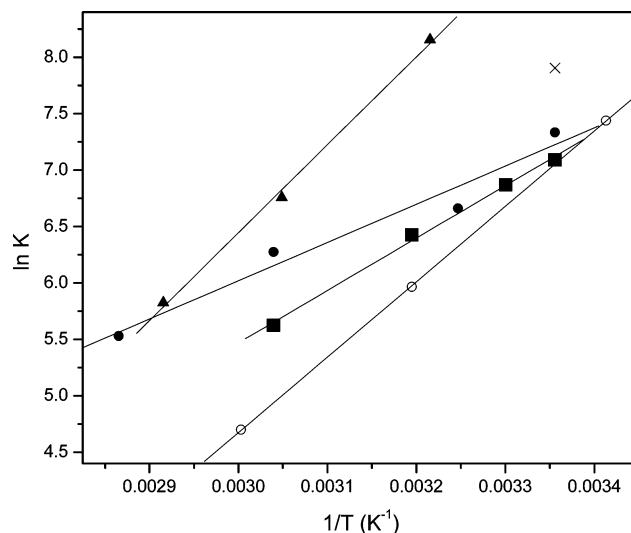
Figure 7. van't Hoff plot of the reaction of NO with $Fe^{II}(EDTA)$. ■: this study. ▲: Hishinuma and Kaji,[11] $[Fe(EDTA)] = 8-36$ mol/m^3, pH = 3–6. ●: Huasheng and Wenchi,[15] $[Fe(EDTA)] = 10-50$ mol/m^3, pH = 5.2–8.2. ×: Schneppensieper et al.,[19–21] $[Fe(EDTA)] = 2$ mol/m^3, pH = 5. ○: Nymoen et al.,[16] $[Fe(EDTA)] = 10-100$ mol/m^3, pH = not mentioned.

ments, $Ha \gg E_A$, and we can safely assume that the absorption process takes place in the instantaneous regime.[23]

The component balance for NO in the gas phase in the stirred cell reactor is

$$V_G\frac{\mathrm{d}C_{A,G}{}^b}{\mathrm{d}t} = F_G(C_{A,G}{}^{in} - C_{A,G}{}^b) - J_A a V_L \tag{25}$$

$$t = 0; \quad C_{A,G}{}^b = 0$$

and for the liquid phase in the stirred cell:

$$V_L\frac{\mathrm{d}C_{AP,L}}{\mathrm{d}t} = J_A a V_L \tag{26}$$

$$t = 0; \quad C_{AP,L} = 0$$

where $C_{AP} = C_A{}^b + C_p{}^b$ is the total amount of absorbed NO. Assuming chemical equilibrium in the liquid phase, we can write:

$$KC_{A,L}{}^b C_{B,L}{}^b = C_{P,L}{}^b \tag{27}$$

$$C_{A,L}{}^b + C_{P,L}{}^b = C_{AP,L}{}^b \tag{28}$$

$$C_{B,L}{}^b = C_{B,L}{}^0 - C_{P,L}{}^b \tag{29}$$

which allows for the calculation of the liquid-phase concentrations once C_{AP} is known.
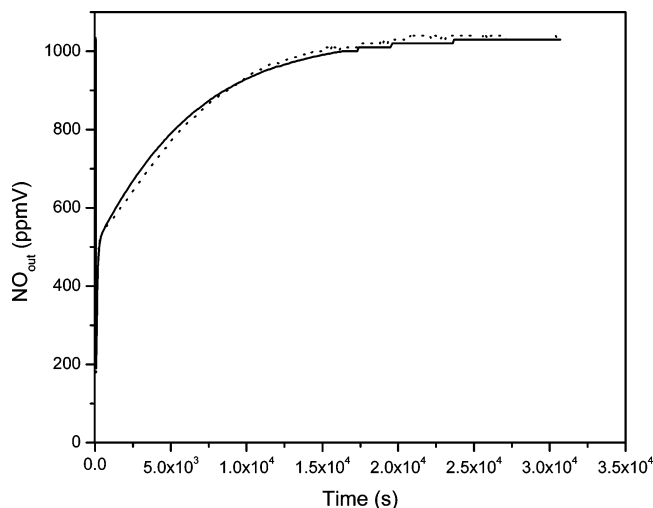
For the mass transfer rate we have:

$$J_A = k_G\left(C_{A,G}{}^b - \frac{C_{A,L}{}^i}{m}\right) \tag{30}$$

and

$$J_A = k_L E_A(C_{A,L}{}^i - C_{A,L}{}^b) \tag{31}$$

where the enhancement factor E_A is given by the

Figure 8. Experimental (dotted line) and modeled (continuous line) absorption profile. Experimental conditions: $T = 299$ K, [Fe(EDTA)] $= 8.1$ mol/m^3, [NO]$_{in} = 1000$ vppm, pH $= 7$.

Figure 9. Comparison of equilibrium constants. $\times$: dynamic reactor modeling (individual fit); $\blacktriangle$: dynamic reactor modeling (simultaneous fit); $\square$: equilibrium approach (see section 5.1). The dotted line represents eq 32.

Figure 10. Temperature dependence of the diffusivity ratio r_P. $\blacksquare$: calculated values of the diffusivity ratio, individual fitting; $\blacktriangle$: calculated values of the diffusivity ratio, simultaneous fitting; $\times$: Demmink.[18] $\bigcirc$: Huasheng and Wenchi.[15]

penetration theory of mass transfer (eq 7) with the assumption $r_P = r_B$.

The set of differential equations (eqs 25 and 26) and the ordinary equations (eqs 27−31) were solved numerically using a fourth order Runge−Kutta method. Parameter estimation was performed using a Newton−Raphson technique.
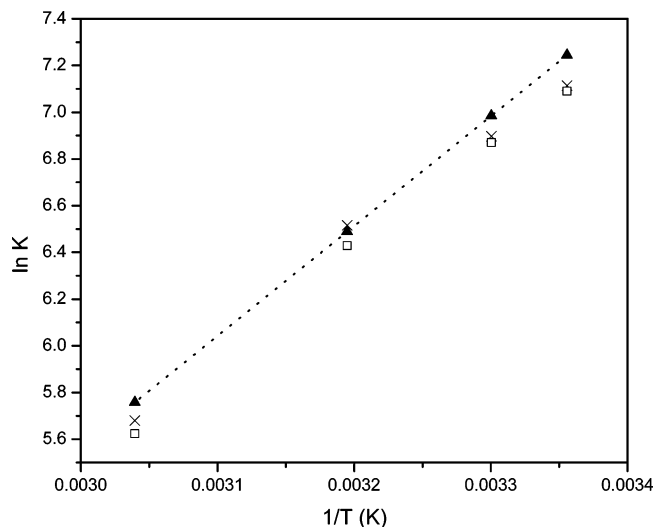
5.3. Parameter Fitting. The two main model parameters are the value of the equilibrium constant (K) and the diffusivity ratio (r_P). Initially, these parameters were fitted for each absorption experiment. Optimization of these parameters using the penetration theory proved very successful, and excellent fits between the measured and modeled absorption profiles were observed. A typical example is given in Figure 8. Attempts to model the profiles using the enhancement factor for the instantaneous regime according to the film theory (eq 6) did not give satisfying results.

A comparison between the equilibrium constants determined using the equilibrium approach and those obtained using the dynamic reactor model is given in Figure 9. Agreement between the K values obtained by the two procedures is very satisfactorily. In a second phase, all absorption experiments were fitted simultaneously. The van't Hoff relation for the temperature dependency of the equilibrium constants was found to be:

$$K = \exp\left(\frac{4702}{T} - 8.534\right) \qquad (32)$$

From this relation, the reaction enthalpy ($\Delta H°$) and entropy ($\Delta S°$) were obtained as −39.1 kJ/mol and −71 J/mol K, respectively.

The values for the diffusivity ratio r$_P$ at various temperatures obtained by simultaneous fitting of all experiments are given in Figure 10. The diffusivity ratio varies between 0.07 and 0.12 and shows slight temperature dependence. There appears to be a maximum at about 315 K, at higher and lower temperatures, the ratio is lower. This trend is likely the result of the very strong temperature dependence of the diffusivity of NO in the aqueous phase. Wise et al.[30] have experimentally determined the diffusion coefficient of various gases in water and found that the diffusivity of NO is showing a very strong temperature dependence. When assuming
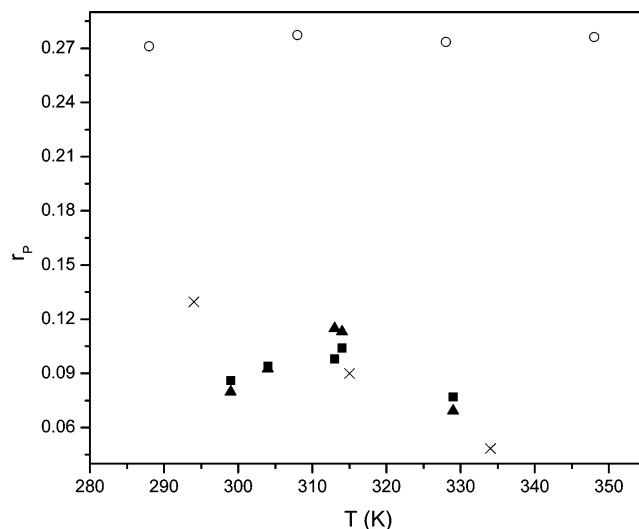
that the temperature dependence of NO is much larger than that of the Fe species, a temperature dependence of the diffusivity ratio (r_P) as given in Figure 10 is expected. The temperature dependence of the diffusivity may be described by the following empirical relation:

$$r_P = -1.775 \times 10^{-4}T^2 + 0.11T - 16.93 \qquad (33)$$

6. Conclusions

The equilibrium constants of the reaction between NO and Fe^{II}(EDTA) in the temperature range 299−329 K, an Fe^{II}(EDTA) concentration of 7−9 mol/m^3, an NO inlet concentration of 1000 vppm, and a fixed pH of 7 at the start of the reaction have been determined. The experiments were carried out in a stirred cell contactor operated batch with respect to the liquid phase and continuously with respect to the gas phase. Two approaches have been applied. In the first approach, experiments were carried out using long reaction times to allow for the establishment of chemical equilibrium

in the setup. The equilibrium constant was determined using the uptake of NO and the $Fe^{II}(EDTA)$ conversion. Second, a dynamic reactor model was developed to describe the experimental absorption profiles. Mass transfer effects were taken into account using the penetration theory for mass transfer. Excellent fits were obtained when assuming that the reaction takes place in the instantaneous regime. The dynamic approach not only allowed calculation of the equilibrium constant of the reaction at various temperatures but also provided accurate data for the diffusivity ratio r_P. Agreement between both approaches was excellent. The results of this study will be valuable input for subsequent experimental and modeling studies to determine the kinetic constants of the relevant reactions in the BiodeNOx process at various process conditions and an optimum BiodeNOx absorber design. These studies will be reported in forthcoming papers.

Acknowledgment

Supporting Information Available: Theory section including equations and references. This material is available free of charge via the Internet at http://pubs.acs.org.

Nomenclature

A_g = salt effect coefficient
a = interfacial area, $m^2 \cdot m^{-3}$
C = concentration, $mol \cdot m^{-3}$
d = diameter gas impeller, m
D = diffusion coefficient, $m^2 \cdot s^{-1}$
E_A = enhancement factor
H = enthalpy, $J \cdot mol^{-1}$
Ha = Hatta number
He = Henry coefficient for solubility, $Pa \cdot m^3 \cdot mol^{-1}$
F = gas flow rate, $m^3 \cdot s^{-1}$
J = molar flux, $mol \cdot m^{-2} \cdot s^{-1}$
K = equilibrium constant, $m^3 \cdot mol^{-1}$
k = mass transfer coefficient, $m \cdot s^{-1}$
$k_{1,1}$ = rate of the reaction, $m^3 \cdot mol^{-1} \cdot s^{-1}$
M = molar weight, $kg \cdot mol^{-1}$
m = solubility = $C_A^i{}_L/C_A^i{}_G$
p = pressure, Pa
$q_A = C_{B,b}/(C_A^i - C_{A,b})$
R = gas constant = $8.314 \ J \cdot mol^{-1} \cdot K$
$r_B = D_B/D_A$, $r_P = D_P/D_A$ = ratio of diffusion coefficients
S = entropy, $J \cdot mol^{-1} \cdot K^{-1}$
T = temperature, Kelvin
t = time, s
V = volume, m^3
W = weight, kg

Greek Symbols

$\alpha = V_G He/V_L RT$
$\beta = C_{B,L}^i/C_{B,L}^b$
Φ = reaction factor
τ = residence time, s

Subscripts

A = component A = NO
AP = component A + P
B = component in the liquid phase
G = gas phase
L = liquid phase
P = product

TOT = total amount
w = water

Superscript

∞ = final
0 = initial value
b = bulk
i = interface
in = inlet
out = outlet
sat = saturation

Literature Cited

(1) Trogler, W. C. The environmental chemistry of trace atmospheric gases. *J. Chem. Educ.* **1995**, *72* (11), 973.

(2) Faucett, H. L.; Maxwell, J. D.; Burnett T. A. *Technical Assessment of NOx Removal Processes for Utility Application: Final Report*; S.I. Electric Power Research Institute, Environmental Protection Agency: Palo Alto, CA, 1978.

(3) *Cost of SCR. Application. Application for NOx Control on Coal-Fired Boilers*; EPA/600/SR-01/087; U.S. Government Printing Office: Washington, DC, 2002.

(4) Chang, S. G.; Littlejohn, D. The potential of a wet process for simultaneous control of SO_2 and NO_x in flue gas. *Prepr. Pap. Div. Fuel Chem.*, *Am. Chem. Soc.* **1998**, *30*, 119.

(5) Hofele, J.; van Helzen, D.; Langenkamp, H.; Schaber, K. Absorption of NO in aqueous solution of $Fe^{II}(NTA)$: determination of the equilibrium constant. *Chem. Eng. Proc.* **1996**, *35*, 295.

(6) Tseng, S.; Babu, M.; Niksa, M.; Coin, R. Electrochemical regeneration of iron chelates for combined NOx and SO_2 removal from combustion gas. *Proceedings of the Intersociety Energy Conversion Engineering Conference*; 1996, Vol. 31, p 1956.

(7) Smith, K. J.; Tseng, S.; Babu, M. Enhanced NOx removal in wet scrubbers using metal chelates. *86th Air and Waste Management Conference*; 1993.

(8) Mendelsohn, M. H.; Harkness, J. B. L. Enhanced flue-gas denitrification using ferrous EDTA and a polyphenolic compound in an aqueous scrubber system. *Energy Fuels* **1991**, *5*, 244.

(9) Buisman, C. J. N; Dijksman, H.; Verbaak, P. C.; den Hartog, A. J. WO Patent No. 96/24434.

(10) Teramoto, M.; Hiramine, S.-I.; Shimada; Y.; Sugimoto, Y.; Terannishi, H. Absorption of dilute monoxide in aqueos solution of Fe(II)−EDTA and mixed solutions of Fe(II)−EDTA and Na_2SO_3. *J. Chem. Eng. Jpn.* **1978**, *11*, 450.

(11) Hishinuma, Y.; Kaji, R. Reversible binding of NO to Fe(II)EDTA. *Bull. Chem. Soc. Jpn.* **1979**, *52* (10), 2863.

(12) Sada, E.; Kumazawa, H.; Kudo, I.; Kondo, T. Individual and simultaneous absorption of dilute NO and SO_2 in aqueous slurries of $MgSO_3$ with Fe(II)−EDTA. *Ind. Eng. Chem. Process Des. Dev.* **1980**, *19*, 377.

(13) Sada, E.; Kumazawa, H.; Takada, Y. Chemical reactions accompanying absorption of NO into aqueous mixed solutions of Fe(II)−EDTA and Na_2SO_3. *Ind. Eng. Chem. Res.* **1984**, *26*, 1468.

(14) Yih, S.-M.; Lii, C.-W. Absorption of NO and SO_2 in Fe-(II)−EDTA solutions I: absorption in a double stirred vessel. *Chem. Eng. Commun.* **1988**, *73*, 43.

(15) Huasheng, L.; Wenchi, F. Kinetics of absorption of nitric oxide in aqueous Fe(II)−EDTA solution. *Ind. Eng. Chem. Res.* **1988**, *27*, 770.

(16) Nymoen, H.; van Velzen, D.; Langekamp, H. Absorption of NO in aqueous solutions of Fe(II)EDTA: determination of the equilibrium constant. *Chem. Eng. Proc.* **1993**, *32*, 9.

(17) Shy, Y.; Littlejohn, D.; Chang, S. Kinetics of NO absorption in aqueous iron(II) bis(2,3-dimercapto-1-propanesulfonate) solutions using a stirred reactor. *Ind. Eng. Chem. Res.* **1996**, *35*, 1668−1672.

(18) Demmink, J. F. Removal of Hydrogen Sulfide and Nitric Oxide with Iron Chelates. Ph.D. Thesis, University of Groningen, The Netherlands, 2000.

(19) Schneppensieper, T.; Finkler, S.; van Eldik, R. Tuning the reversible binding of NO to iron(II) amynocarboxylate and related complexes in aqueous solution. *Eur. J. Inorg. Chem.* **2001**, 491.

(20) Schneppensieper, T.; Wanat, A.; Stochel, G.; Goldstein, S.; Meyerstein, D.; Van Eldik, R. Ligand effect of the kinetics of the reversible binding of NO to selected aminocarboxilato complexes of iron(II) in aqueous solution. *Eur. J. Inorg. Chem.* **2001**, 2317.

(21) Schneppensieper, T.; Wanat, A.; Stochel, G.; Van Eldik, R. Mechanistic information on the reversible binding of NO to selected iron(II) chelates from activation parameters *Inorg. Chem.* **2002**, *41*, 2565−2573

(22) Vogel, A. I. *Vogel's Textbook of Quantitative Chemical Analysis*; Longman: Harlow, England, 1978.

(23) Westerterp, K. R.; van Swaaij, W. P. M.; Beenackers, A. A. C. M. *Chemical Reactor Design and Operation*; Wiley: New York, 1984.

(24) Onda, K.; Sada, E.; Kobayashi, T.; Fujine, M. Gas absorption accompanied by complex chemical reactions—reversible chemical reactions. *Chem. Eng. Sci.* **1970**, *25*, 753.

(25) De Coursey, W. J.; Thring R. W. Effect of unequal diffusivities on enhancement factors for reversible and irreversible reaction. *Chem. Eng. Sci.* **1989**, *44*, 1715.

(26) Winkelman, J. G. M.; Brodsky, S. J.; Beenackers, A. A. C. M. Effects of unequal diffusivities on enhancement factors for reversible reactions: numerical solutions and comparison with DeCoursey's method. *Chem. Eng. Sci. Commun.* **1992**, *47* (2), 485.

(27) Versteeg, G. F.; van Swaaij, W. P. M. Solubility and diffusivity of acid gases (CO_2, N_2O) in aqueous alkanolamine solutions. *J. Chem. Eng. Data* **1988**, *33*, 29.

(28) Fogg, P. G. T.; Gerrard, W. *Solubility of Gases in Liquids*; Wiley: New York, 1990.

(29) Wubs, H. J. Application of Iron Chelates in Hydrodesulphurisation. Ph.D. Thesis, University of Groningen, The Netherlands, 1994.

(30) Wise, D. L.; Houghton, G. Diffusion coefficients of neon, krypton, xenon, carbon monoxide and nitric oxide in water at 10−60 °C. *Chem. Eng. Sci.* **1968**, *23*, 1211.

(31) Ho, C. S.; Ju, L.-K.; Baddour R. F.; Wang, D. I. C. Simultaneous measurements of oxygen diffusion coefficients and solubilities in electrolyte solutions with a polarographic oxygen electrode. *Chem. Eng. Sci.* **1990**, *43*, 3093.

(32) Winkelman, J. G. M.; Voorwinde, O. K.; Ottens, M.; Beenackers, A. A. C. M.; Janssen, L. P. B. M. Kinetics and chemical equilibrium of the hydration of formaldehyde. *Chem. Eng. Sci.* **2002**, *57*, 4067.

(33) Janssen, L. P. B. M.; Warmoeskerken, M. M. C. G *Transport Phenomena Data Companion*; Delftse Universitaire: Pers, The Netherlands, 1987.

(34) Reid, R. C.; Prausnitz, J. M.; Poling, B. E. *Properties of Gases and Liquids*; McGraw-Hill: New York, 1987.